

# Trapping and Release of Citrate-Capped Gold Nanoparticles

*Darwin R. Reyes,<sup>†\*</sup> Geraldine I. Mijares,<sup>†</sup> Brian Nablo,<sup>†</sup> Kimberly A. Briggman,<sup>‡</sup> and Michael Gaitan<sup>†</sup>*

<sup>†</sup>Semiconductor Electronics Division, EEEL, and <sup>‡</sup>Optical Technology Division, Physics Laboratory,  
National Institute of Standards and Technology, Gaithersburg, Maryland 20899

\*Corresponding author: Darwin R. Reyes; darwin.reyes@nist.gov

Telephone: 301-975-5466, Fax: 301-975-5668.

An electrical method to trap and release charged gold nanoparticles onto and from the surface of gold electrodes modified by an alkanethiol self-assembled monolayer (SAM) is presented. To form electrodes coated with gold nanoparticles (GNPs), amine-terminated SAMs on gold electrodes were immersed in a solution of negatively charged citrate-capped GNPs. Accumulation of GNPs on the electrode surface was monitored by a decrease in the impedance of the SAM-modified electrode and by an increase in the electrochemical activity at the electrode as shown through cyclic voltammetry (CV). Electrostatic interactions between the GNPs and the amine-terminated SAM trap the GNPs on the electrode surface. Application of a subsequent negative bias to the electrode initiated a partial release of the GNPs from the electrode surface. Impedance spectroscopy, cyclic voltammetry, ultraviolet-visible (UV-Vis) spectroscopy and AFM imaging were used to monitor and confirm the attraction of GNPs to and release from the aminealkanethiolated gold electrodes. This work describes a method of trapping and release for citrate-capped GNPs that could be used for on-demand nanoparticle delivery

applications such as in assessing and modeling nanoparticle toxicology, as well as for monitoring the functionalization of gold nanoparticles.

## 1. INTRODUCTION

The unique electrical and optical properties of engineered metal nanoparticles have prompted the use of these materials in commercial products as well as in a continuously increasing number of research studies aimed at developing new technological applications that span from high-throughput screening applications to cellular imaging [(1); (2)]. The nature of these unique properties is such that, with a small change in size, shape, or degree of nanoparticle agglomeration, a large change in the wavelength of maximum absorption ( $\Delta\lambda_{\text{max}} \approx \text{few hundred nm}$ ) as well as in particle charging energies (of a few hundred mV) can be exerted [(3)]. In opposition to these properties, nanoparticles exhibit similar surface modification chemistries as bulk metal surfaces, allowing nanoparticles to be functionalized with similar methods as their bulk counterparts. Although much has been done to study the physicochemical characteristics of nanoparticles for future biomedical applications, the data regarding the toxicological effects on living cells has been inconsistent [(4)]. This inconsistency may be attributed in part to varying conditions the nanoparticles are exposed to when presented to cells *in vitro*. The agglomeration of metal nanoparticles can change with time and media composition, which presents difficulty in trying to account for the differences in cytotoxicity of nanoparticles of different sizes and shapes. In order to better understand the physicochemical characteristics of aqueous suspensions of nanoparticles (e.g., surface charge, size, and degree of agglomeration) and how they interact with themselves and the environment, new technological approaches are needed. Advanced control of nanoparticle delivery will provide toxicologists with better tools to quantify and control the exposure of nanoparticles in biological environments.

Electronic methods of particle manipulation have several advantages over other methods, such as the entrapment of nanoparticles in a polymeric resin [(5)], the use of optical manipulation [(6)], and

electrophoresis deposition assisted by laser trapping [(7)]. One benefit of electronically controlled release of nanoparticles includes the capability of assembling a massively parallel, dense array of microelectrodes for independent manipulation. This type of arrangement is particularly useful for repeated exposure to cells or when multiple analyses or conditions are desired. Micron-sized electrodes allow for the integration of these nanoparticle delivery systems into microfluidic networks, which also provides advantageous integration and parallelization. Electronic methods such as dielectrophoresis (DEP) have previously been used as a manipulation technique for nanoparticles. In most of the cases, the nanoparticles are brought to the gap between two electrodes using either DEP or electrostatic trapping to further use the trapped nanoparticles as nanowires [(8); (9); (10); (11)]. However, DEP requires very small gaps (one to seven times the size of the nanoparticle) to attract the nanoparticles to the electrodes [(12; 13)]. These gap dimensions require specialized equipment such as electron-beam lithography to produce. On the other hand, electrodes for electrostatic trapping can be fabricated at the micrometer size and therefore do not require specialized equipment to produce.

Gold nanoparticles (GNPs) are commonly capped with a stabilizing agent that prevents them from getting in contact with each other. In particular, citrate as a capping agent imparts a negative charge to GNPs, which in turn repulses adjacent nanoparticles and prevents them from agglomerating. Citrate is a common stabilizing agent since GNPs can be synthesized through a citric acid reduction reaction [(14; 15)]. The negative charge imparted by the citrate capping on GNPs could be used to attract the modified GNPs to oppositely charged materials. For example, negatively charged GNP surfaces were recently used as a discriminator for chymotrypsin substrates. [(16-19)] By orienting the active site of chymotrypsin toward the negatively charged GNP, negatively charged substrates could not reach the active site of the enzyme, whereas positively charged substrates could be converted into their products. Others have immobilized citrate-stabilized GNPs by electrostatic attraction on aminoalkanethiols and their electroreflectance studied [(20-22)]. In this work, we take advantage of the negative charge of citrate-capped GNPs to attract and then controllably release GNPs from aminoalkanethiol-modified gold

electrodes by changing the potential bias of the electrode. The GNPs are attracted to the aminoalkanethiol surfaces by simple electrostatic interactions between the negatively charged citrate groups on GNPs and the positively charged amino groups on the SAM. Release of GNPs is achieved by applying a negative bias at the modified gold electrodes. The trapping and release of GNPs is monitored by a variety of techniques, including impedance spectroscopy, cyclic voltammetry (CV), ultraviolet-visible (UV-Vis) spectroscopy and AFM imaging.

## **2. Material and methods**

2.1. Fabrication of gold electrodes. Thin gold films were deposited onto Pyrex glass wafers (Bullen Ultrasonics, Inc., Eaton, OH). A titanium-tungsten film (TiW, Kurt J. Lesker, Co., Pittsburg, PA), 3 nm to 4 nm thick, was first sputtered to serve as an adhesion layer for the gold [(23)], then a gold layer was deposited. The thickness of the gold layer was either 50 nm for UV-VIS analysis to allow for optical transparency or 200nm for infrared (IR) analysis to provide complete IR reflectivity. 2.2. Modification of gold electrodes with aminoalkanethiol SAMs. A solution of 1.0 mM 11-amino-1-undecanethiol, hydrochloride (Dojindo Molecular Technologies, Inc., Rockville, MD) was prepared in 10 % v/v ammonium hydroxide balanced with ethanol. Gold electrodes were first cleaned by UV-ozone exposure in a UV-ozone cleaner (Jelight Company, Inc., Irvine, CA) and then immediately placed in contact with the alkanethiol solution for times ranging from 5 min to 24 h to monitor SAM completion via IR analysis. A PDMS reservoir was used to contain the alkanethiol solution in a specific area of the gold electrodes. After each self-assembly period, the SAM was rinsed with ethanol, 10 % acetic acid, and ethanol to rinse away potential accumulated multilayers of the SAM prior to IR or CV analysis.

2.3. Trapping and release of GNPs. GNPs spontaneously assembled onto aminoalkanethiol-modified electrodes in a  $9 \times 10^{10}$  particles/mL solution of 40 nm gold nanoparticles (Nanocs, Inc., New York, NY). The modified gold electrode, as well as the counter and reference electrodes, was connected to a Solartron 1260 Impedance/Gain-Phase Analyzer with a Solartron SI 1287A Electrochemical Interface

(Solartron Analytical, Oak Ridge, TN). The impedance was monitored throughout the duration of the GNP assembly period. The release of GNPs from the electrode surface was carried out by applying a negative DC bias of 0.5 V versus Ag/AgCl in 3 periods of 10 s each. *In situ* CV and impedance measurements were taken between each release period to monitor the degree of release.

2.4. Preparation of GNP-free supernatant (background) samples. GNP (40 nm) solutions were transferred to a 2 mL tube and centrifuged at 13,000 RPM for 10 min (Eppendorf, Hauppauge, NY). The supernatant was transferred to a new tube and centrifuged again at 13,000 RPM for another 10 min. The supernatant was analyzed using UV-Vis spectroscopy to observe the decrease in absorbance when the gold nanoparticles were removed from the solution thus generating a GNP-free solution. The GNP-free solution was then transferred to the electrochemical cell where the impedance and CV measurements were performed during the trapping and release periods.

2.5. Impedance Spectroscopy and Cyclic Voltammetry. The AC signal used to characterize the impedance was 40 mV peak-to-peak over the frequency range of 1 Hz to  $10^6$  Hz. A three electrode system was used for both impedance and voltammetric measurements. The modified gold electrode was used as the working electrode, a Pt wire was the counter electrode, and a Ag/AgCl electrode served as the reference electrode. Impedance measurements were taken before and during the immersion of the working electrode into the GNP solution. CV measurements were acquired in phosphate buffer saline (PBS) solution, pH 7.4. The change in impedance was monitored for up to 18 h during the GNP trapping period. The CV scans were obtained by cycling between - 0.5 and 0.5 V at 100 mV/s. The impedance spectra and CV curves were recorded using the ZPlot2/ZView2 and CorrWare/CorrView software packages (Scribner Associates, Inc., Southern Pines, NC), respectively.

2.6. UV-Vis Spectroscopy. UV-Vis spectra of the GNPs in solution were obtained using a NanoDrop 1000 (Thermo Scientific, Wilmington, DE). *In situ* UV-Vis spectra of the GNPs on the modified gold electrodes were taken in transmission using a Lambda 45 spectrometer (Perkin Elmer, Waltham, MA).

2.7. IR Absorption Spectroscopy. IR spectra of the aminoalkanethiolate monolayers were acquired with

4  $\text{cm}^{-1}$  resolution in an  $85^\circ$  reflection geometry using a ThermoNicolet Nexus 670 FT-IR (Thermo Electron Corporation, Madison, WI) to monitor the uptake of the aminoalkanethiolate SAM.

2.8. Atomic Force Microscopy (AFM). AFM images (Dimension 5000, Digital Instruments, Santa Barbara, CA) were attained in tapping mode using the Nanoscope (R) III software. Uncoated silicon tips with a typical radius of curvature of 10 nm were used (Mikro Masch, San Jose, CA). Images were acquired at ambient conditions on dry samples. Heights were measured at the center of the particles.

### 3. RESULTS AND DISCUSSION

Self-assembly of the 11-amino-1-undecanethiol (aminoalkanethiol) monolayer on the planar gold electrodes was monitored using IR spectroscopy and CV (Supporting Figure S1). The IR spectra show the uptake of the SAM during the formation of the aminoalkanethiolate SAM on the gold surface as a function of time (Supporting Figure S1A). The IR data show the progression of the SAM uptake process from 5 min to 24 h. The IR peak observed at  $2850\text{ cm}^{-1}$  corresponds to the C-H symmetric stretch of  $\text{CH}_2$  groups on the surface and is used to monitor the SAM formation. A nearly complete SAM was observed after 5 min of immersion as evidenced by the lack of intensity change of the  $2850\text{ cm}^{-1}$  IR peak after this time (Supporting Figure S1B). Gold electrodes were immersed in the aminoalkanethiol solution for approximately 1 h for the remainder of the study. An absorption peak observed at  $2962\text{ cm}^{-1}$  corresponds to a  $\text{CH}_3$  group, likely the result of contamination by PDMS, which was used as a barrier to contain the aminoalkanethiol solution and not fully rinsed away. However, the PDMS contamination did not appear to influence the aminoalkanethiolate monolayer formation.

The quality of SAM formation on planar gold surfaces was also evaluated with CV. After the gold was exposed to the aminoalkanethiol for 1 h, the electrochemical activity of the gold surface decreased considerably, as anticipated (Figure 1). The background current dropped in some regions of the CV curve, by more than an order of magnitude, demonstrating the complete coverage of the gold surface with the aminoalkanethiolate SAM.

To confirm the influence of the presence of GNPs, a GNP-free supernatant (background) solution was created as described in the Materials and Methods section. Figure 2 shows the change in absorbance for the blank samples generated from the GNP solutions by a sequential centrifugation procedure. After the first centrifugation step most of the GNPs formed a pellet at the bottom of the tube. The absorbance reached almost the baseline level of zero. The second centrifugation rendered the sample with an absorbance at the same level as the water (used as the blank). This shows that virtually no nanoparticles remain in the solution used as the GNP-free supernatant.

The entrapment of GNPs occurs by immersing the SAM-modified planar gold into a solution of citrate-capped GNPs. The positively charged amine groups of the SAM electrostatically attract the negatively charged citrate-capped GNPs. This interaction causes a change in impedance, with the greatest difference observed over 1.5 h to 2 h. Therefore, the experiments were conducted within this time frame. Figure 3 shows the change in impedance when the SAM-modified gold electrodes were immersed in a GNP solution and GNP supernatant of a centrifuged GNP solution. The largest differences in impedance of these two exposures are observed to occur between 1 Hz and 100 Hz. When comparing the changes in impedance for both graphs at 10 Hz ( $t = 0$  and  $t = 120$  min), the difference in impedance for the GNP solution was approx. 4 times more (798 ohms for the GNP solution versus 196 ohms for the supernatant solution) when compared to the GNP-free supernatant solution. This change could be due to an increase in the active surface area of the modified gold electrode occurring while the GNPs continuously anchor onto the modified electrode.

Cyclic voltammetry was also used to monitor the attraction of GNPs onto the modified gold electrode surface (Figure 4). The CV of SAM-modified electrodes demonstrated only a small change when immersed in the GNP-free supernatant solution (Figure 4A), in contrast to being exposed to the GNP solution (Figure 4B), which resulted in a significant increase in the background current. Additionally, the three electrochemical reactions observed in the bare gold electrode CV plots reappeared, although shifted to higher potentials (Figure 1C and Figure 4B). The marked change in the CV plot when the

modified electrodes are immersed for 2 h in the GNP solution shows that the GNPs were responsible for restoring electrochemical activity to the SAM-modified electrode.

Tapping mode AFM images acquired in air confirmed that the GNPs were firmly adhered to the SAM-modified gold electrode after 2 h of incubation in the GNP solution. Figure 5 shows an image ( $1\ \mu\text{m} \times 1\ \mu\text{m}$ ) of an aminoalkanethiol modified gold electrode with 5 GNPs present. Individual line scans depicted an average height for the GNPs of  $37 \pm 2\ \text{nm}$ .

An extended applied potential of  $-0.5\ \text{V}$  versus Ag/AgCl is observed to induce the release of GNPs from the surface of the SAM-modified gold. The release of GNPs was done in three 10 s pulses of  $-0.5\ \text{V}$  each. The effect of the releasing potential was monitored using cyclic voltammetry, UV-Vis spectroscopy, and AFM imaging.

Figure 6 shows the CV of modified electrodes after the negative bias was applied. Figure 6 shows the CVs of the electrode immersed in a GNP-free supernatant solution before and after a negative bias was applied. Only negligible changes in the CVs of the SAM-modified electrodes exposed to the GNP-free supernatant solution were observed after the application of the  $-0.5\ \text{mV}$  bias. Conversely, a SAM-modified electrode immersed in the GNP solution displayed a reduction in the background current after each 10 s pulse of the negative bias. This trend is consistent with the assertion that GNPs are being released when a negative bias is applied.

UV-Vis spectroscopy of the electrodes before and after the release of GNPs was performed to corroborate the results from the CV plots. Figure 6 shows the UV-Vis spectrum of GNPs in solution (Fig. 7A), the spectra of GNP bound to SAM-modified gold electrodes after 2 h of trapping (Fig. 7B), and after the GNP releasing step (Fig. 7C). These spectra show a maximum absorption of GNPs in solution at 533 nm as well as on the modified gold electrode surface. After the baseline normalization of the surface immobilized GNP samples, nearly half of the absorbance at 533 nm is lost after applying the pulsed negative voltage releasing steps, suggesting that the GNPs detached when a negative bias was applied.

The detachment of the GNPs after an applied negative potential was further confirmed with tapping mode AFM imaging. Supporting figure S2 shows an image of GNPs adhered onto a SAM-modified gold electrode after a 2 h trapping period (left panel). After applying the negative bias (right panel), the number of GNPs on the surface notably decreased. This is consistent the results obtained with the impedance spectroscopy, CV and UV-Vis spectroscopy.

#### **4. CONCLUSIONS**

This work presents a simple electronic method for the trapping and controlled release of gold nanoparticles. We record that properties of aminoalkanethiolate-modified gold electrodes change when in contact with citrate-capped GNPs via impedance spectroscopy, cyclic voltammetry, and UV-Vis spectroscopy. All measurements agree in terms of the assembly of the GNPs on the electrode. The presence of the GNPs decreased the impedance of the SAM-modified electrode and increased the electrochemical activity at the electrode as shown through CV. After the application of a - 0.5 V, negative bias, an increase in impedance and a decrease in electrochemical activity were observed, which suggests the GNPs were being released from the electrode surface. AFM images provided visual evidence that many of the GNPs were released from the SAM-modified electrodes after the negative bias was applied. This approach could be used for on-demand nanoparticle delivery applications such as in assessing and modeling nanoparticle toxicology, as well as for monitoring the functionalization of gold nanoparticles.

#### **ACKNOWLEDGMENT**

This work was supported by the NIST Innovations in Measurement Science Cellular Biometrology Program. Electrode fabrication was performed at the NIST Center for Nanoscale Science and Technology Nanofabrication facility in Gaithersburg, MD.

## REFERENCES

- [1] S.J. Park, T.A. Taton, C.A. Mirkin, *Science* 295 (2002) 1503-1506.
- [2] I.H. El-Sayed, X.H. Huang, M.A. El-Sayed, *Nano Letters* 5 (2005) 829-834.
- [3] W.P. McConnell, J.P. Novak, L.C. Brousseau, R.R. Fuieler, R.C. Tenent, D.L. Feldheim, *Journal of Physical Chemistry B* 104 (2000) 8925-8930.
- [4] Y. Pan, S. Neuss, A. Leifert, M. Fischler, F. Wen, U. Simon, G. Schmid, W. Brandau, W. Jahnen-Dechent, *Small* 3 (2007) 1941-1949.
- [5] O. Abed, M. Wanunu, A. Vaskevich, R. Arad-Yellin, A. Shanzer, I. Rubinstein, *Chemistry of Materials* 18 (2006) 1247-1260.
- [6] A.H.J. Yang, S.D. Moore, B.S. Schmidt, M. Klug, M. Lipson, D. Erickson, *Nature* 457 (2009) 71-75.
- [7] F. Iwata, M. Kaji, A. Suzuki, S. Ito, H. Nakao, *Nanotechnology* 20 (2009).
- [8] K.D. Hermanson, S.O. Lumsdon, J.P. Williams, E.W. Kaler, O.D. Velev, *Science* 294 (2001) 1082-1086.
- [9] R. Kretschmer, W. Fritzsche, *Langmuir* 20 (2004) 11797-11801.
- [10] A. Bezryadin, C. Dekker, G. Schmid, *Applied Physics Letters* 71 (1997) 1273-1275.
- [11] I. Amlani, A.M. Rawlett, L.A. Nagahara, R.K. Tsui, *Applied Physics Letters* 80 (2002) 2761-2763.
- [12] R.J. Barsotti, M.D. Vahey, R. Wartena, Y.M. Chiang, J. Voldman, F. Stellacci, *Small* 3 (2007) 488-499.
- [13] D. Cheon, S. Kumar, G.H. Kim, *Applied Physics Letters* 96 (2010).
- [14] J. Turkevich, P.C. Stevenson, J. Hillier, *Discussions of the Faraday Society* (1951) 55-&.
- [15] J. Turkevich, P.C. Stevenson, J. Hillier, *Journal of Physical Chemistry* 57 (1953) 670-673.
- [16] N.O. Fischer, C.M. McIntosh, J.M. Simard, V.M. Rotello, *Proceedings of the National Academy*

of Sciences of the United States of America 99 (2002) 5018-5023.

[17] R. Hong, N.O. Fischer, A. Verma, C.M. Goodman, T. Emrick, V.M. Rotello, *Journal of the American Chemical Society* 126 (2004) 739-743.

[18] C.C. You, M. De, G. Han, V.M. Rotello, *Journal of the American Chemical Society* 127 (2005) 12873-12881.

[19] C.C. You, M. De, V.M. Rotello, *Organic Letters* 7 (2005) 5685-5688.

[20] T. Baum, D. Bethell, M. Brust, D.J. Schiffrin, *Langmuir* 15 (1999) 866-871.

[21] D. Bethell, M. Brust, D.J. Schiffrin, C. Kiely, *Journal of Electroanalytical Chemistry* 409 (1996) 137-143.

[22] T. Sagara, N. Kato, N. Kakashima, *Journal of Physical Chemistry B* 106 (2002) 1205-1212.

[23] Certain commercial equipment, or materials are identified in this paper to foster understanding. Such identification does not imply recommendation or endorsement by the National Institute of Standards and Technology, nor does it imply that the materials or equipment are necessarily the best available for the purpose.

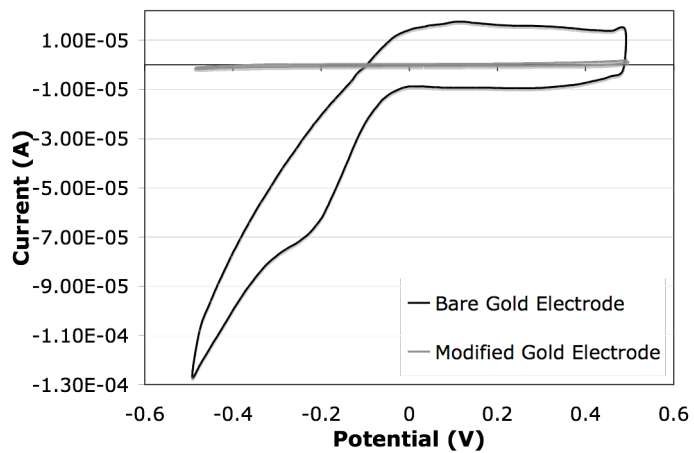


Figure 1. CV plots of a bare gold electrode and an aminoalkanethiol-modified gold electrode. Note the difference in background current once the gold surface is covered with the aminoalkanethiol.

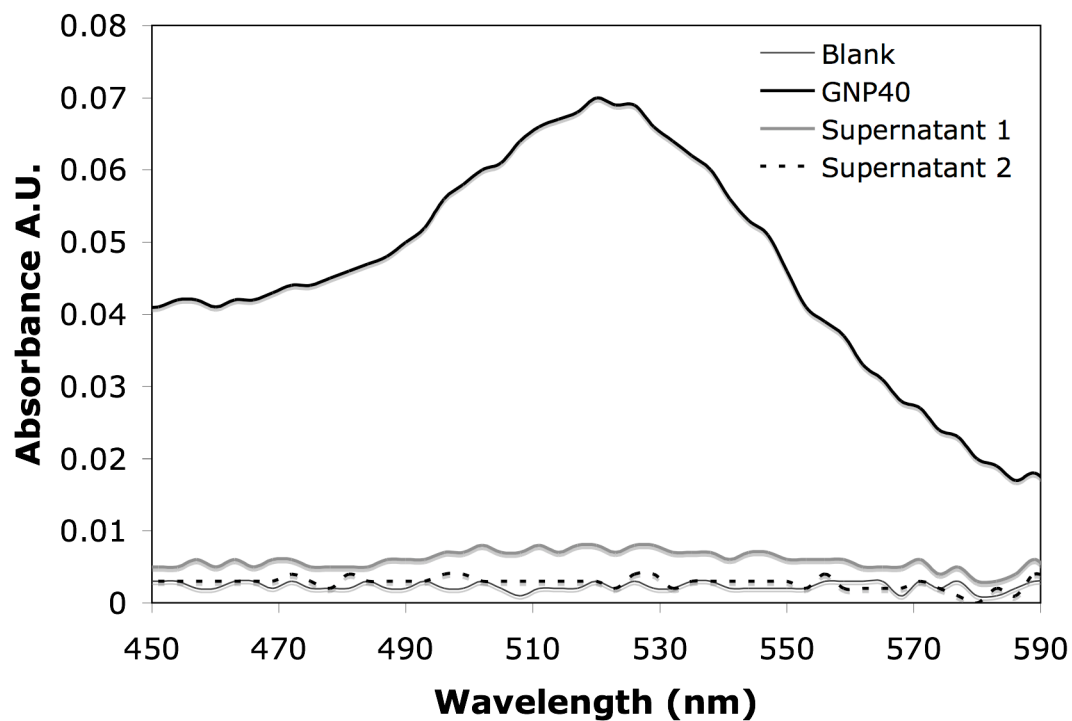


Figure 2. UV-Vis spectra of the decrease of gold nanoparticles in solution with two-step centrifugation to obtain a GNP-free supernatant solution. The absorbance of the gold nanoparticle solution (GNP40), after the first centrifugation (Supernatant 1) and after the second centrifugation (Supernatant 2) decreased with the sequential centrifugations used to remove the GNP40 from the solution.

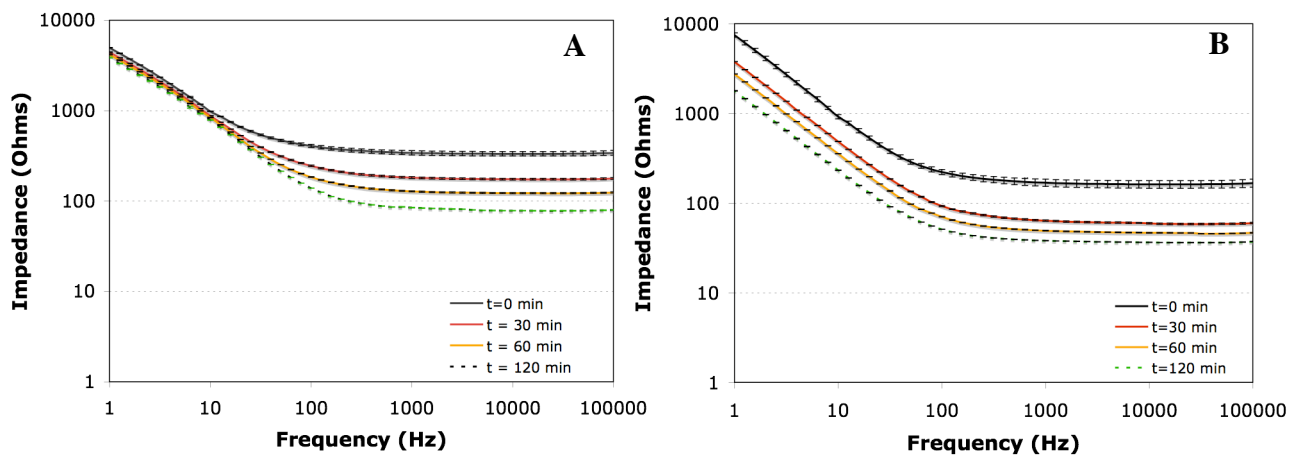


Figure 3. Change in impedance of the modified gold electrodes as a function of time. Plot of impedance as a function of frequency when an aminoalkanethiol-modified gold electrode is immersed in (A) GNP-free supernatant solution and (B) GNP solution. The changes occurring at the surface of the electrodes are observed at low frequencies. Error bars are the standard deviations of three measurements for each point in the curves.

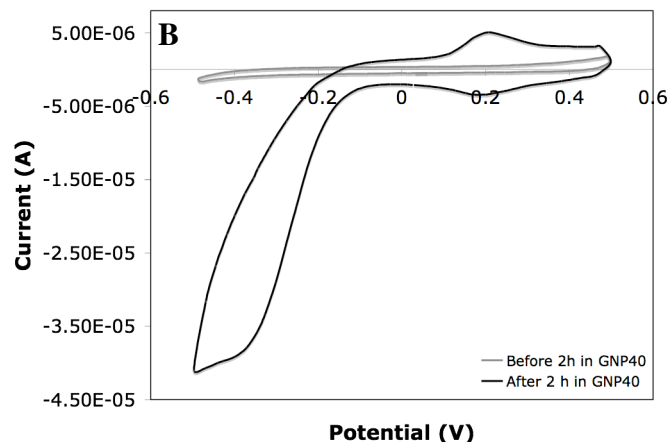
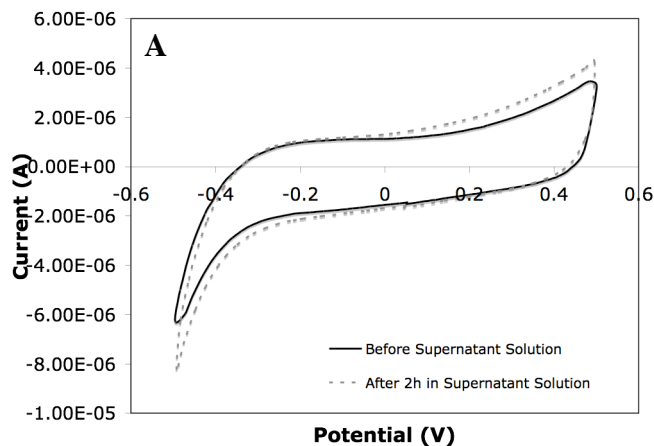


Figure 4. CV plots of supernatant and GNP solutions. Cyclic voltammograms show the response of the aminoalkanethiol-modified gold electrodes when immersed in the GNP supernatant solution (A) and when immersed in the GNP solution (B). The supernatant solution shows no background current before and after immersion in supernatant solution, whereas a change in background current is observed when the aminoalkanethiol-modified gold electrode is immersed in the GNP solution. CV measurements were taken in phosphate buffer saline (PBS) solution, pH 7.4.

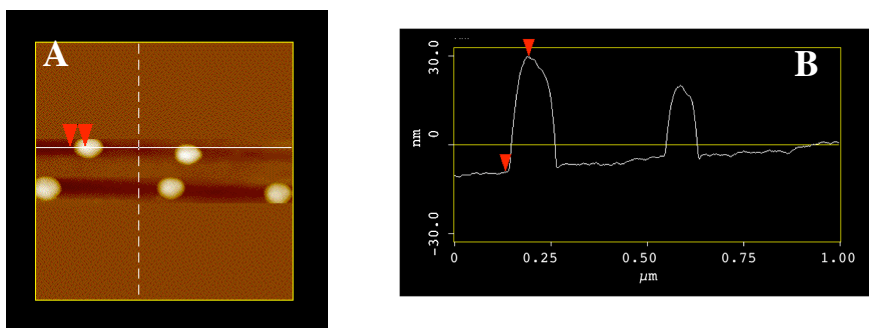


Figure 5. (A) AFM image ( $1 \mu\text{m} \times 1 \mu\text{m}$ ) of 40 nm GNPs bound to aminoalkanethiol-modified gold electrodes. (B) AFM section analysis showing a vertical distance of 39 nm from the baseline to the highest point of the curve (see red arrows). The average vertical distance of the GNPs shown in this image is  $37 \pm 2 \text{ nm}$ .

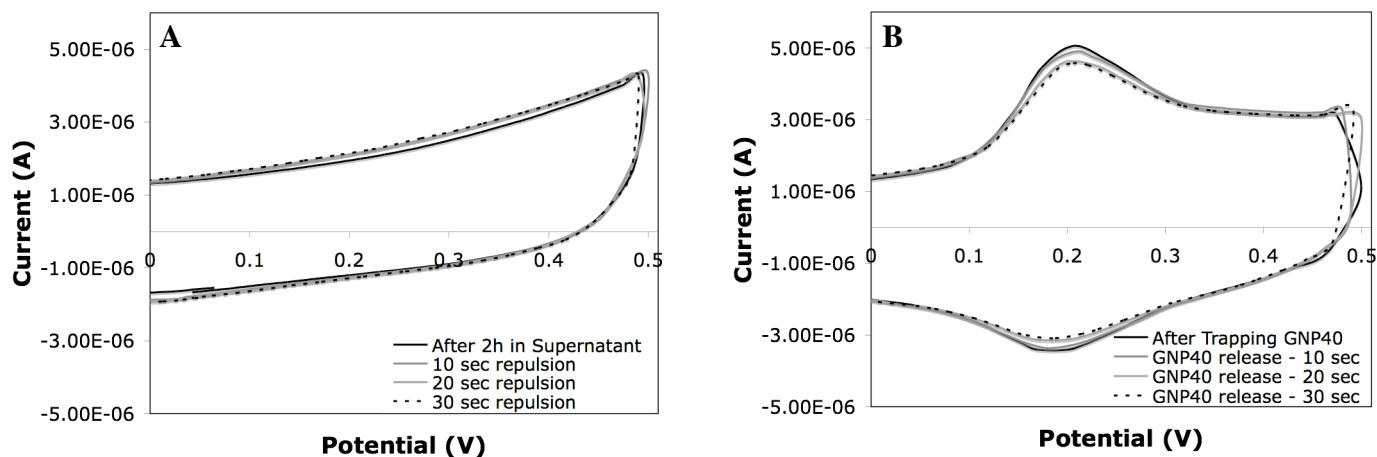


Figure 6. Cyclic voltammograms for the GNP release steps. (A) The aminoalkanethiol-modified gold electrode immersed in GNP supernatant solution shows a flat background current after 2 h in the supernatant solution. It remains virtually the same after three releasing periods of applied voltage (-0.5 V) versus Ag/AgCl electrode. (B) The aminoalkanethiol-modified gold electrode immersed in the GNP solution for 2 h shows an increase in the overall background current and a decrease in peak current with each applied voltage period (10 seconds each, -0.5 V versus Ag/AgCl).

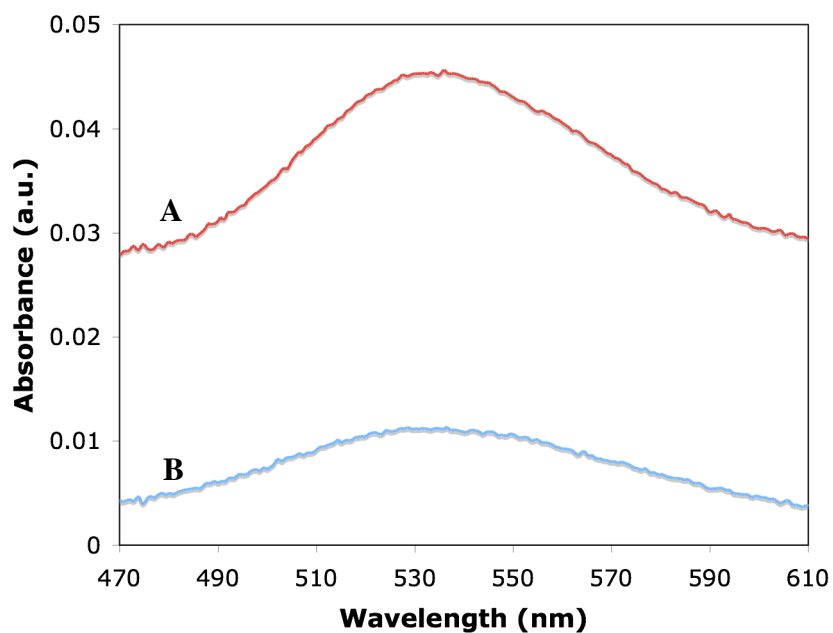
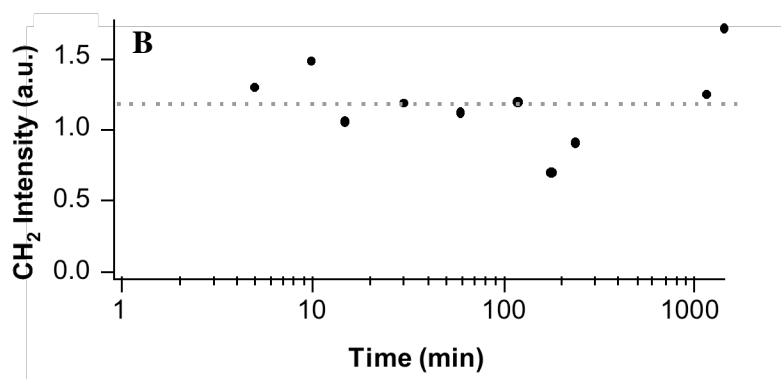
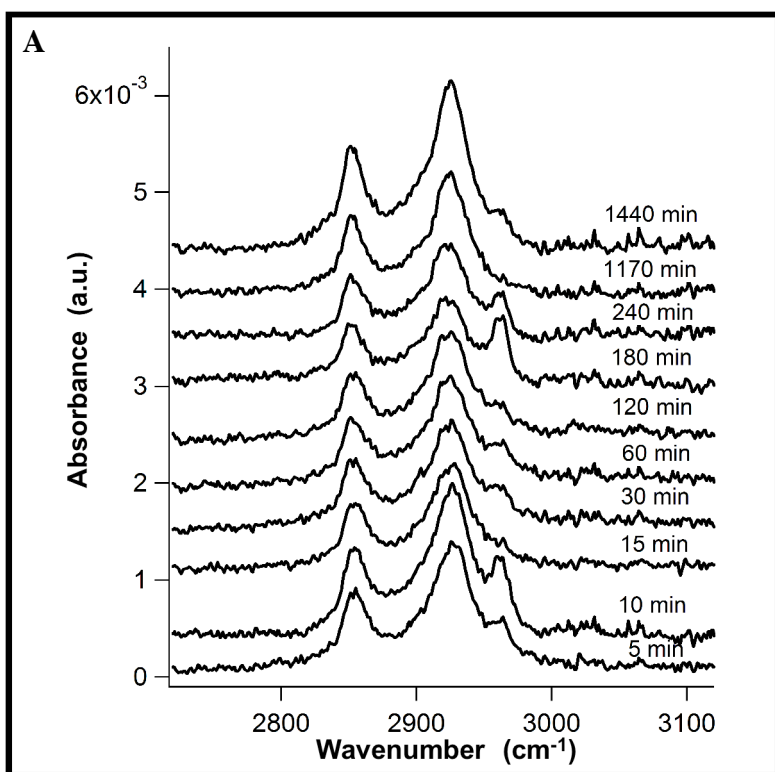
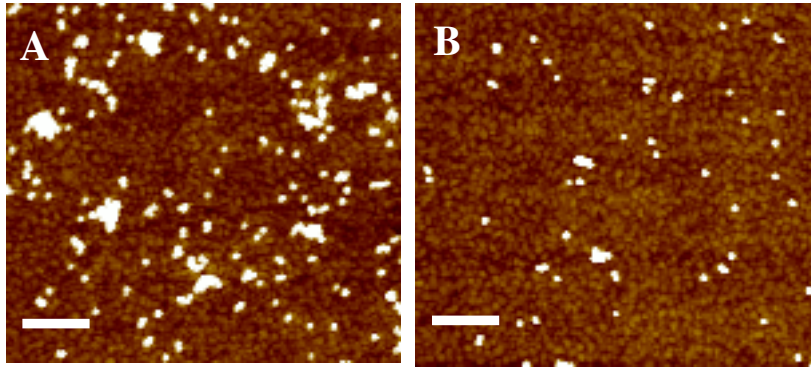


Figure 6. UV-Vis spectra of GNPs. (A) GNPs adsorbed on aminoalkanethiol-modified gold electrode after the trapping period of 2 h. (B) Remaining GNPs adsorbed on aminoalkanethiol-modified gold electrode after applying a voltage of -0.5 V versus Ag/AgCl (releasing period).



Supporting Figure S1. A) IR spectra monitoring aminoalkanethiolate SAM formation with 11-amino-1-undecanethiol on gold surfaces as a function of time. Spectra are offset for clarity. The  $2850 \text{ cm}^{-1}$  peak correspond to  $(\text{CH}_2)$  groups used to monitor the formation of the SAM. B) Plot of  $\text{CH}_2$  intensity at  $2850 \text{ cm}^{-1}$  for the time points used in A). This plot illustrates the formation of only one layer of aminoalkanethiolate on the gold surfaces.



Supporting Figure S2. Atomic force microscopy images of GNPs. A) An illustration of an area showing GNPs bound onto the SAM-modified gold electrode after the trapping period, and B) an area showing the aminoalkanethiol-modified gold electrode after the release of GNPs period. Notice the difference in number of GNPs before the release and after the release period. In these examples the difference is approximately an order of magnitude between the number of cells trapped and the number of cells retained ( $\sim 226$  GNPs trapped vs.  $\sim 20$  GNPs retained). Scale bar: 500 nm.